

Are your MRI contrast agents cost-effective?

Learn more about generic Gadolinium-Based Contrast Agents.



FRESENIUS
KABI

caring for life

AJNR

**Combined Diffusion Tensor Imaging and
Apparent Transverse Relaxation Rate
Differentiate Parkinson Disease and Atypical
Parkinsonism**

G. Du, M.M. Lewis, S. Kanekar, N.W. Sterling, L. He, L.
Kong, R. Li and X. Huang

This information is current as
of April 17, 2024.

AJNR Am J Neuroradiol published online 31 March 2017
<http://www.ajnr.org/content/early/2017/03/30/ajnr.A5136>

Combined Diffusion Tensor Imaging and Apparent Transverse Relaxation Rate Differentiate Parkinson Disease and Atypical Parkinsonism

 G. Du,  M.M. Lewis,  S. Kanekar,  N.W. Sterling,  L. He,  L. Kong,  R. Li, and  X. Huang



ABSTRACT

BACKGROUND AND PURPOSE: Both diffusion tensor imaging and the apparent transverse relaxation rate have shown promise in differentiating Parkinson disease from atypical parkinsonism (particularly multiple system atrophy and progressive supranuclear palsy). The objective of the study was to assess the ability of DTI, the apparent transverse relaxation rate, and their combination for differentiating Parkinson disease, multiple system atrophy, progressive supranuclear palsy, and controls.

MATERIALS AND METHODS: A total of 106 subjects (36 controls, 35 patients with Parkinson disease, 16 with multiple system atrophy, and 19 with progressive supranuclear palsy) were included. DTI and the apparent transverse relaxation rate measures from the striatal, midbrain, limbic, and cerebellar regions were obtained and compared among groups. The discrimination performance of DTI and the apparent transverse relaxation rate among groups was assessed by using Elastic-Net machine learning and receiver operating characteristic curve analysis.

RESULTS: Compared with controls, patients with Parkinson disease showed significant apparent transverse relaxation rate differences in the red nucleus. Compared to those with Parkinson disease, patients with both multiple system atrophy and progressive supranuclear palsy showed more widespread changes, extending from the midbrain to striatal and cerebellar structures. The pattern of changes, however, was different between the 2 groups. For instance, patients with multiple system atrophy showed decreased fractional anisotropy and an increased apparent transverse relaxation rate in the subthalamic nucleus, whereas patients with progressive supranuclear palsy showed an increased mean diffusivity in the hippocampus. Combined, DTI and the apparent transverse relaxation rate were significantly better than DTI or the apparent transverse relaxation rate alone in separating controls from those with Parkinson disease/multiple system atrophy/progressive supranuclear palsy; controls from those with Parkinson disease; those with Parkinson disease from those with multiple system atrophy/progressive supranuclear palsy; and those with Parkinson disease from those with multiple system atrophy; but not those with Parkinson disease from those with progressive supranuclear palsy, or those with multiple system atrophy from those with progressive supranuclear palsy.

CONCLUSIONS: DTI and the apparent transverse relaxation rate provide different but complementary information for different parkinsonisms. Combined DTI and apparent transverse relaxation rate may be a superior marker for the differential diagnosis of parkinsonisms.

ABBREVIATIONS: CN = caudate nucleus; FA = fractional anisotropy; MD = mean diffusivity; MoCA = Montreal Cognitive Assessment; MSA = multiple system atrophy; MSA-P = MSA parkinsonian subtype; PD = Parkinson disease; PSP = progressive supranuclear palsy; PUT = putamen; R2* = apparent transverse relaxation rate; ROC = receiver operating characteristic; RN = red nucleus; SN = substantia nigra; STN = subthalamic nucleus; UPDRS-III = Unified Parkinson's Disease Rating Scale, Part III (motor part)

Parkinson disease (PD), multiple system atrophy (MSA), and progressive supranuclear palsy (PSP) are the 3 most common parkinsonian syndromes with overlapping clinical manifestations.

Differentiating these diseases on the basis of clinical symptoms alone can be challenging.^{1,2} Despite similar clinical symptoms, each


Received September 22, 2016; accepted after revision January 11, 2017.

From the Departments of Neurology (G.D., M.M.L., N.W.S., L.H., X.H.), Radiology (S.K., X.H.), Pharmacology (M.M.L., X.H.), Neurosurgery (X.H.), Kinesiology (X.H.), Bioengineering (X.H.), and Public Health Sciences (L.K.), Pennsylvania State University—Milton S. Hershey Medical Center, Hershey, Pennsylvania; Department of Public Health (L.H.), Shanxi Medical University, Taiyuan, China; and Department of Statistics (R.L.), Pennsylvania State University, University Park, Pennsylvania.


This work was supported in part by the National Institute of Neurological Disorders and Stroke (NS082151), the Hershey Medical Center General Clinical Research Center (National Center for Research Resources, grant ULI RR033184, which is now at the Na-

tional Center for Advancing Translational Sciences, grant ULI TR000127), the National Institute on Drug Abuse (P50 DA039838 and P50 DA036107), the National Nature Science Foundation of China (11690014 and 11690015), the Pennsylvania Department of Health Tobacco CURE Funds, the Michael J. Fox Foundation for Parkinson's Research, the Alzheimer's Association, Alzheimer's Research UK, and the Weston Brain Institute.

Please address correspondence to Guangwei Du, MD, PhD, Department of Neurology, 500 University Dr, Hershey, PA 17033; e-mail: guangweidu@hmc.psu.edu; Xue-mei Huang, MD, PhD, Department of Neurology, 500 University Dr, Hershey, PA 17033; e-mail: xuemei@psu.edu

 Indicates open access to non-subscribers at www.ajnr.org

 Indicates article with supplemental on-line appendix and table.

 Indicates article with supplemental on-line photos.

<http://dx.doi.org/10.3174/ajnr.A5136>

disorder has distinct gross and microscopic pathologies. PD is marked by the loss of dopamine neurons in the substantia nigra (SN).³ MSA is characterized neuropathologically by glial and neuronal cytoplasmic inclusions in many basal ganglia and cerebellar related structures,⁴ whereas PSP has neuronal loss, gliosis, and neurofibrillary tangles in both the basal ganglia and cerebellum that may extend to limbic areas.^{5,6}

Two MR imaging modalities, diffusion tensor imaging and the apparent transverse relaxation rate ($R2^*$), have been studied intensively in recent decades with the goal of detecting the distinct pathologic patterns in PD, MSA, and PSP and differentiating them from each other.⁷⁻¹³ DTI has been suggested to reflect the disruption of microstructural integrity (eg, cell death and associated myelin changes), whereas $R2^*$ has been used to estimate iron accumulation in brain tissue.^{14,15} There has been little effort, however, to directly compare DTI and $R2^*$ in the differential diagnosis of PD and atypical parkinsonism, and in testing whether they can provide complementary information regarding pathology and/or discriminability of those diseases.^{10,14}

In the current study, we compared the pattern of DTI and $R2^*$ changes among the different parkinsonian diseases and a control group in multiple ROIs that included striatal-, midbrain-, limbic-, and cerebellar-related structures. The performance of DTI, $R2^*$, and their combination to discriminate controls from patient groups and patient groups from each other also was assessed by using an Elastic-Net machine learning approach with a nested 10-fold cross-validation.

MATERIALS AND METHODS

Subjects

A total of 106 individuals (16 with MSA parkinsonian subtype [MSA-P], 19 with PSP [13 with Richardson subtype and 6 with parkinsonian subtype], 35 with PD, and 36 healthy controls) were included in this study from an ongoing longitudinal case-control cohort established in 2012. Patients were recruited from a tertiary movement disorders clinic, and controls were recruited from the spouse population of the clinic or the local community. All patients were free of major neurologic/medical issues other than PD, MSA-P, or PSP, and all controls were free of any known neurologic/psychiatric diagnoses. Patient diagnoses were initially established according to published criteria¹⁶⁻¹⁸ by a movement disorder specialist and updated (August 2016) before the analysis of the current data according to the most recent clinical assessment and postmortem pathology if available (5 PD and 3 PSP cases were confirmed by postmortem pathology results). Two subjects (1 with PD and 1 with PSP) were excluded from later analyses due to severe motion artifacts. Disease duration was defined as the number of years between the date when a parkinsonian syndrome was first diagnosed by a medical professional and the study visit date. All participants were administered the Movement Disorder Society Unified Parkinson's Disease Rating Scale part III (UPDRS-III) for motor function assessment and the Montreal Cognitive Assessment (MoCA) for global cognitive function.¹⁹ UPDRS-III and MoCA scores and MR imaging scans were collected for patients in an "on" state. The study was approved by the institutional review board at the Pennsylvania State University-Milton S. Hershey Medical Center. All subjects provided written informed consent.

MR Imaging Data Acquisition

Brain MRIs were obtained from all participants by using a 3T MR imaging system (Magnetom Trio; Siemens, Erlangen, Germany) with an 8-channel phased array head coil. The MR imaging examination included multi-gradient-echo (for $R2^*$) and diffusion tensor imaging sequences, along with high-resolution T1-weighted and T2-weighted images for segmentation. Detailed imaging parameters are described in the On-line Appendix.

DTI and $R2^*$ Maps

Diffusion tensor images were processed using DTIPrep (Neuro Image Research and Analysis Laboratory, University of North Carolina, Chapel Hill, North Carolina). In DTIPrep, a thorough quality control for diffusion-weighted images was performed by intersection and intervolume correlation analysis, eddy currents, and motion artifact correction. Fractional anisotropy (FA) and mean diffusivity (MD) maps were then estimated for subsequent analysis.

For $R2^*$, an affine registration was used to align 6 magnitude images to an averaged mean magnitude image for potential head motion correction in multi-gradient-echo images. The $R2^*$ maps then were generated by using a voxelwise nonlinear Levenberg-Marquardt algorithm to fit a monoexponential function ($s = s_0 e^{-TE \times R2^*}$) by using an in-house Matlab (MathWorks, Natick, Massachusetts) tool.

ROI Segmentation

The segmentation of ROIs was performed by using the Advanced Normalization Tools software package (ANTs; <http://stnava.github.io/ANTs/>)²⁰ and an atlas-based segmentation pipeline implemented in AutoSeg (<http://www.nitrc.org/projects/autoseg/>),²¹ along with an in-house atlas. An unbiased, age-appropriate template was generated from T1-weighted images from all controls with ANTs.²² The following 13 ROIs, including striatal and related structures (putamen [PUT], caudate nucleus [CN], and globus pallidus), midbrain (anterior SN, posterior SN, red nucleus [RN], and subthalamic nucleus [STN]), limbic (hippocampus and amygdala), and cerebellar structures (dentate nucleus, cerebellar hemisphere, superior cerebellar peduncle, and middle cerebellar peduncle) were defined on the cohort-specific T1-weighted and T2-weighted templates by an experienced neuroimager (G.D.). Segmented ROIs are illustrated in On-line Fig 1. ROIs for each subject were then parcellated by using AutoSeg with ANTs as a warping option^{21,23} (see the On-line Appendix for details regarding the segmentation process). On-line Fig 3 illustrates the segmentation quality for small structures (SN, RN, and superior cerebellar peduncle).

B0 images for DTI and mean magnitude images for $R2^*$ then were coregistered to individual T2-weighted images using ANTs. The resulting transformations were then applied to FA, MD, and $R2^*$ maps by using a B-spline interpolation to bring FA, MD, and $R2^*$ images into the same space as the segmented ROIs, where the mean values of FA, MD, and $R2^*$ for each ROI were calculated for subsequent analyses.

Statistical Analysis and Modeling

The difference in sex frequency among groups was evaluated by using the χ^2 test. Age and disease duration were compared by using 1-way analysis of variance. MoCA and UPDRS-III scores

Table 1: Demographic and clinical data for control and patient groups^a

	Control	PD	MSA-P	PSP	P Value
No. of subjects	36	35	16	19	
Female/male	13:23	12:23	8:8	4:15	.356 ^b
Age (yr)	70.0 ± 7.5	70.3 ± 7.9	68.0 ± 7.5	74.9 ± 8.7	.057 ^c
Disease duration (yr)	–	3.4 ± 3.6	3.9 ± 3.3	3.2 ± 2.8	.812 ^c
MoCA	25 ± 2.3	22.8 ± 4.5	23.9 ± 2.7	20.1 ± 4.9	.002, ^d .120 ^e
UPDRS III	4.6 ± 3.6	36.6 ± 27.3	51.5 ± 20.0	46.6 ± 23.4	<.0001, ^d .145 ^e

^aData are sums or mean ± SD.

^bGroup difference in sex was compared among all 4 groups using the χ^2 test.

^cGroup differences in age and disease duration were compared using 1-way ANOVA.

^dGroup differences in MoCA and UPDRS-III were compared among all 4 groups using ANCOVA with adjustments for age and sex.

^eGroup differences in MoCA and UPDRS-III were compared among the 3 patient groups, using ANCOVA with adjustments for age and sex.

among groups were assessed by using 1-way analyses of covariance with adjustments for age and sex.

Each MR imaging measurement in patients with PD, MSA-P, and PSP was compared with that of controls by using univariate ANCOVAs with age and sex as covariates for each of the 13 ROIs. For MR imaging measurements, the Bonferroni method was used to correct for multiple comparisons, with a resulting *P* value ≤ .0038 (0.05/13 independent tests) considered significant.

One major challenge for multimodal MR imaging studies is the high dimensionality of potential predictors generated from different MR imaging measurements and brain structures, which can result in overfitting and collinearity among variables, causing traditional analyses to fail. In this study, we used an Elastic Net regularized logistic regression approach with a nested 10-fold cross-validation scheme to unravel the high-dimensional problem. Two hyperparameters need to be defined in Elastic-Net regularized regression. In our study, α was fixed to 0.2 empirically and λ was selected by an inner layer 10-fold cross-validation that was independent of the outer layer 10-fold cross-validation used for performance evaluation. This nested cross-validation setting was implemented to alleviate potential overfitting.²⁴

Regularized logistic models were built from all ROI measurements including R2*, DTI (including both FA and MD), and the combined measures (R2*, FA, and MD) for discriminating the following: 1) controls from those with PD/MSA-P/PSP, 2) those with PD from those with MSA-P/PSP, 3) controls from those with PD, 4) those with PD from those with MSA-P, 5) those with PD from those with PSP, and 6) those with MSA-P from those with PSP. Receiver operating characteristic (ROC) curves were generated by using outer layer 10-fold cross-validation models for each MR imaging technique and their combination. A bootstrap approach was used to test the differences among ROC curves.²⁵ ROC curve comparisons were performed between the combined marker and DTI because DTI was better or equal to R2* in all 6 scenarios mentioned above. Sensitivity, specificity, positive predictive value, and negative predictive value were generated by using the Youden method.

Statistical analyses were performed by using the open-source statistical software package R (Version 3.0.3; <http://www.r-project.org>). Elastic-Net regularized logistic regression was conducted by using the R package glmnet (http://web.stanford.edu/~hastie/glmnet/glmnet_alpha.html),²⁶ whereas the ROC curve

analyses were performed by using the R package pROC (<https://cran.r-project.org/web/packages/pROC/index.html>).²⁷

RESULTS

Demographic Data

Demographic characteristics for subjects are shown in Table 1. No significant overall differences in sex distribution or age were detected among the control, PD, PSP, and MSA-P groups. Post hoc pair-wise analysis showed trending differences between MSA-P and PSP in both sex (*P* = .072) and age (*P* = .065).

Thus, both age and sex were entered as covariates for group comparisons. Logistic regression on age and sex showed no comparable discriminability among PD, MSA-P, and PSP (area under the curve < 0.66). Although patients had significantly lower MoCA and higher UPDRS-III scores compared with controls, there were no significant differences among the patient groups on the clinical measures (disease duration, MoCA, or UPDRS-III).

DTI and R2* Comparison between Parkinsonian Disease and Control Groups

Compared with controls, patients with PD showed changes in the posterior SN and RN in both DTI and R2*, though only the R2* value in the RN survived correction for multicomparesions. Patients with both MSA and PSP showed more widespread changes (after correction for multicomparesions) involving structures both within and outside the midbrain. The pattern of changes, however, was different between the 2 groups. Namely, patients with MSA-P showed increased MD values in the PUT, globus pallidus, cerebellum, and middle cerebellar peduncle, a decreased FA value in the STN, and increased R2* values in the STN and middle cerebellar peduncle. Patients with PSP, however, showed increased MD and R2* values in the posterior substantia nigra but no changes in the STN or any other basal ganglia structures. Patients with PSP had significantly increased MD values in the dentate nucleus, cerebellum, and superior cerebellar peduncle, but not in the middle cerebellar peduncle (Table 2 and On-line Table).

Discriminative Analysis

We compared the discriminative ability of DTI and R2* measures and their combination under 6 different scenarios by using Elastic-Net regularized logistic regression and ROC curves (Table 3 and On-line Fig 2). The combined models (DTI+R2*) were better than DTI or R2* alone (*P*s < .05) in discriminating controls from those with PD/MSA-P/PSP, controls from those with PD, those with PD from those with MSA-P/PSP, and those with PD from those with MSA-P. When we considered the separation of controls from subjects with PD, the combined model was improved dramatically compared with either measure alone (from area under the curve = 0.82 to area under the curve = 0.91, *P* = .001).

The DTI model, however, showed strong discriminability when differentiating PD from PSP (area under the curve = 0.97) or MSA-P from PSP (area under the curve = 0.96), and adding R2* did not significantly improve the performance of the model. Nevertheless, R2* alone showed decent discriminative ability

Table 2: Individual MRI measurements in PD, MSA-P, and PSP compared with controls in different structures

	PD			MSA-P			PSP		
	FA	MD	R2*	FA	MD	R2*	FA	MD	R2*
Striatal and related structures									
PUT					↑ ↑ ^a			↑	
CN									
GP					↑ ↑ ↑ ^a	↑	↑	↑	
Midbrain structures									
antSN				↓		↑		↑ ↑	↑
postSN	↓ ↓	↑	↑ ↑	↓ ↓		↑		↑ ↑ ↑ ↑ ^a	↑ ↑ ↑
RN			↑ ↑ ^a	↓ ↓	↑			↑	↑ ↑ ↑
STN				↓ ↓ ^a	↑	↑ ↑ ↑ ^a			↑
Limbic structures									
Hipp							↓	↑ ↑ ↑ ↑ ^a	↓
AM				↓			↓	↑ ↑	
Cerebellar structures									
DN							↓	↑ ↑ ^a	
CB				↓ ↓	↑ ↑ ↑ ^a		↓ ↓ ↓ ^a	↑ ↑ ^a	
SCP							↓ ↓ ↓ ↓ ^a	↑ ↑ ↑ ↑ ^a	
MCP				↓	↑ ↑ ↑ ^a	↓ ↓ ↓ ^a		↑ ↑ ^a	↑ ↑

Note:—antSN indicates anterior substantia nigra; postSN, posterior substantia nigra; Hipp, hippocampus; AM, amygdala; CB, cerebellum; DN, dentate nucleus; GP, globus pallidus; MCP, middle cerebellar peduncle; SCP, superior cerebellar peduncle.

^a Statistical significance after Bonferroni correction ($P < .0038$, considering 13 independent tests). Upward arrows indicate increased MRI measures compared with controls, and downward arrows indicate decreased MRI measures compared with controls. ↑ represents $P < .05$, ↑ ↑ represents $P < .01$, ↑ ↑ ↑ represents $P < .001$, and ↑ ↑ ↑ ↑ represents $P < 0.0001$.

Table 3: ROC analysis of individual and combined MRI modalities

	AUC	Sens	Spec	PPV	NPV	P Value ^a
C vs PD/MSA-P/PSP						.013
DTI + R2*	0.88	0.80	0.83	0.82	0.81	
DTI ^b	0.80	0.81	0.71	0.60	0.87	
R2*	0.75	0.69	0.69	0.55	0.81	
C vs PD						.001
DTI + R2*	0.91	0.86	0.80	0.82	0.89	
DTI	0.82	0.74	0.76	0.75	0.76	
R2*	0.78	0.71	0.75	0.71	0.74	
PD vs MSA-P/PSP						.038
DTI + R2*	0.94	0.86	0.87	0.88	0.84	
DTI	0.89	0.83	0.80	0.82	0.81	
R2*	0.87	0.87	0.77	0.87	0.77	
PD vs MSA-P						.006
DTI + R2*	0.99	0.97	1.00	1.00	0.93	
DTI	0.89	0.83	0.86	0.79	0.86	
R2*	0.91	0.86	0.86	0.94	0.70	
PD vs PSP						.156
DTI + R2*	0.99	0.97	1.00	1.00	0.94	
DTI	0.97	0.94	0.94	0.97	0.89	
R2*	0.87	0.80	0.83	0.82	0.81	
MSA-P vs PSP						.435
DTI + R2*	0.98	0.94	1.00	1.00	0.93	
DTI	0.96	0.94	0.92	0.94	0.92	
R2*	0.89	0.86	0.80	0.82	0.81	

Note:—Sens indicates sensitivity; Spec, specificity; PPV, positive predictive value; NPV, negative predictive value; AUC, area under the curve; C, controls.

^a ROC curves were compared between the models, including all MRI measurements and that with DTI measurements only.

^b Models for DTI measurements were generated by including both FA and MD features.

when differentiating PD from PSP (area under the curve = 0.87) and MSA-P from PSP (area under the curve = 0.89).

DISCUSSION

First, we confirmed that DTI and R2* differentiate parkinsonian syndromes and controls. In addition, our studies demonstrated that DTI and R2* can capture the distinct pathologic patterns of the different parkinsonian syndromes and may pro-

vide complementary information about each disease. Individually, DTI showed better discriminability among the disease groups, whereas R2 added significant value in separating controls from those with parkinsonian syndromes and those with PD from those with MSA-P/PSP or MSA-P.

DTI and R2* Changes in PD

The pathologic hallmark of PD is neuronal loss in the SN pars compacta. Our study may capture this pathology by demonstrating decreased FA and increased R2* in the posterior SN.^{28,29} The inclusion of additional ROIs in our study, however, requires a rather conservative Bonferroni correction; thus, the detected difference did not reach statistical significance. Future studies are needed to confirm these findings in light of a recent meta-analysis suggesting that nigral FA changes in patients with PD vary widely.³⁰ In the current study, patients with PD also demonstrated increased R2* values in the RN. This result is consistent with the notion that the RN may be involved in the primary cerebellar motor pathway, which has been shown to be affected in PD.^{31,32}

DTI and R2* Changes in MSA-P

We also found significantly increased MD values in the PUT, globus pallidus, cerebellum, and middle cerebellar peduncle of patients with MSA-P, consistent with previous neuroimaging results.^{7,8,12,33,34} On the basis of previous studies, DTI MD changes in the CN have been controversial. For example, Seppi et al³⁵ reported significantly increased MD values in the CN, whereas others have found no changes in CN MD values.^{12,34} We did not find significant MD changes in the CN, consistent with these later reports. One study reported MD changes in the SN of patients with MSA-P¹²; however, we could not replicate this finding. Pathology studies have reported robust changes in the PUT but more variable changes in other basal ganglia regions.^{4,36} This varying pathology may contribute partly to the inconsistent DTI findings in the CN and SN in the current study and previous ones.^{9,12,13,34,35}

Patients with MSA-P consistently demonstrated increased R2* values in the PUT.¹⁰⁻¹² The current study, however, failed to detect R2* changes in the PUT of these patients. Although the exact reason for the discrepancy is unknown, we postulate the following 2 possibilities: First, heterogeneous cohort characteristics may have contributed to the different results. For example, previous studies had significantly younger patients with MSA (mean ages, 58–62 years) compared with our cohort (mean age, 68 years). Age significantly affects iron and R2* values in basal ganglia structures.³⁷ Thus, these age effects may mask the disease-related changes in the PUT. Second, the different R2* techniques used among the studies may influence the results.^{10,12,38} For example, Lee et al¹¹ used 8 echoes and a TR = 24 ms, whereas Barbagallo et al¹² used 6 echoes with repetition and a TR = 100 ms; and we used 6 echoes and a TR = 54 ms. In addition to imaging parameters, each study used different curve-fitting techniques: Lee et al¹¹ used linear fitting after log-transformation of the original signal, whereas the current study used nonlinear curve-fitting to a mono-exponential function similar to that in Barbagallo et al.¹²

Most interesting, we detected a decreased FA value in the STN of patients with MSA-P, along with an increased R2* value, which has not been reported by any previous MR imaging studies, to our knowledge. It is unclear whether the lack of significant STN findings arises from a lack of focus on this structure or whether no differences were found. The neuronal/glial cytoplasmic inclusions that typically are found in basal ganglia regions are less common in the STN of patients with MSA.⁴ One pathology study, however, noted increased microglia in the STN of patients with MSA-P,³⁶ which may reflect a reactive or compensatory process instead of the primary pathology. Thus, the STN changes we detected may reflect these reactive or compensatory changes, though future studies focused on the STN are warranted to verify this.

DTI and R2* Changes in PSP

Consistent with previous studies, we found significant DTI (MD) changes in midbrain (posterior SN and cerebellar [cerebellum and superior cerebellar peduncle]) structures of patients with PSP, with the most robust change seen in the superior cerebellar peduncle.^{7,8,35,39} Whereas most studies reported increased MD values in the PUT of patients with PSP,^{35,39,40} we did not detect MD changes in the PUT or other basal ganglia structures (CN and globus pallidus) in the current study. Consistent with our findings, Tsukamoto et al³⁴ reported no MD changes in the PUT of patients with PSP. Additional studies are needed to clarify the discrepancies.

In the past, both pathologic and neuroimaging studies with free-water imaging suggested changes in the STN of patients with PSP.^{6,13} Pathologic studies also reported both neuronal and oligodendroglia loss in the STN of patients with PSP. Using traditional DTI measures (FA and MD), the current study did not detect significant changes in the STN of patients with PSP. It is possible that the mixed microscopic pathology may have complex or opposing effects on these traditional DTI measurements at the macroscopic level. Change in the STN of patients with PSP by means of the free-water measure derived from a bi-tensor model¹³ suggests that free-water may be a more sensitive marker for PSP-related pathology in the STN. Future studies are needed

to further confirm the links between PSP-related pathology and different MR imaging contrasts.

In the current study, we also detected an increased MD value in the dentate nucleus of patients with PSP. Although this finding is new, it is in line with pathologic results of neuronal loss in the dentate nucleus of patients with PSP.⁶ In addition, patients with PSP demonstrated significantly increased MD values in the hippocampus and a trending change in the amygdala. These results are consistent with previous volumetric studies suggesting pathologic involvement of the hippocampus in PSP^{5,41} and early cognitive issues that often are detected in patients with PSP clinically. These findings are inconsistent, however, with previous pathologic studies indicating that the hippocampus and amygdala are spared from τ pathology in patients with PSP.⁴² A growing literature supports the heterogeneity of PSP and mixed pathologic findings across different tauopathies^{39,43}; thus, the value of using differential imaging patterns to subtype the patient with PSP will be evaluated in the future.

Previous studies on R2* in the PUT, CN, and globus pallidus in patients with PSP have been controversial because some studies showed significantly increased R2* values in these structures,^{11,44} whereas others did not.¹⁰ The current results are consistent with no R2* changes in the PUT, CN, and globus pallidus. Patients with PSP, however, had significantly increased R2* values in the SN and RN. This finding is consistent with previous PSP pathologic studies indicating that τ pathology-related neuronal and oligodendroglia loss is involved in both the SN and RN.⁴²

Discriminative Analysis

Many promising MR imaging markers have been suggested to differentiate patients with PD from those with atypical parkinsonism.^{8,9,13,45,46} Systematic comparison and validation of those markers in the same subjects are needed before translating these findings into a clinical setting. The current study is the first to systematically compare DTI, R2*, and their combination by using Elastic-Net regularized logistic regression. When we compared DTI and R2* measures under 6 clinically relevant scenarios, our results suggested the following: 1) that DTI measures overall are better or comparable with R2* values in differentiating parkinsonisms, and 2) that R2* provides complementary information in most scenarios except when differentiating PD from PSP or MSA-P from PSP.

Limitations

The current study has some limitations. First, among 70 patients with parkinsonism, only 8 cases were confirmed by postmortem pathology. Despite updating the clinical diagnosis by integrating more longitudinal clinical information right before conducting the current analysis, diagnosis error inevitably exists and might bias the results. Additionally, we included controls with positive UPDRS-III scores as high as 14. It is possible that controls with high UPDRS-III scores have a preclinical parkinsonian syndrome. Nonetheless, a recent study has demonstrated that parkinsonian signs are common in older adults, even without a clinical diagnosis of disease.⁴⁷ Second, this study is case-control in nature and does not simulate clinical practice, which would include other diseases potentially confused with PD such as essential tremor,

corticobasal degeneration, dementia with Lewy bodies, and psychogenic disorders. In addition, we did not separate PSP subtypes.⁴³ Re-analyzing the data to include only patients with PSP Richardson subtype ($n = 13$) did not change the results demonstrably from those including the entire PSP cohort. Finally, in the current study, all data were collected while patients were on anti-parkinsonian medications, and the MR imaging measures may be affected by the drugs. Further prospective studies that mimic clinical practice are warranted to further test the potential of these markers in clinical practice.

Technically, recent advances in MR imaging markers for PD and atypical parkinsonism have suggested that 2 new measures (free-water and quantitative susceptibility) may be useful for discriminating patient groups and are derived from the same MR imaging data (DTI and $R2^*$, respectively). Quantitative susceptibility has been suggested to improve the $R2^*$ signal by reducing potential confounders of the iron measurement,⁴⁸ whereas free-water may provide additional information above traditional FA or MD values.⁴⁹ The current study did not include these new measures, and future work validating and comparing them is warranted. Finally, this study did not compare our models with conventional MR imaging clues used by radiologists in these disorders, such as the “hummingbird” and “hot cross bun” signs, midbrain atrophy, and putaminal T2-weighted hypointensity.⁵⁰⁻⁵² Notably, Reiter et al,⁵¹ with visual rating of dorsolateral nigral hyperintensity in susceptibility-weighted images, showed promising discriminability in differentiating those with parkinsonian syndromes from controls. It will be important to discern the additional value a quantitative MR imaging marker derived from combining DTI and $R2^*$ provides compared with the best medical knowledge. In this study, we adopted an Elastic-Net regularized regression as the multivariate classification method. Even though we used a nested 10-fold cross-validation for model selection and performance evaluation, the models still may be overly optimistic due to the small sample size.²⁴

CONCLUSIONS

Our findings are consistent with those in previous neuroimaging and postmortem pathologic studies reporting significant involvement of striatal-, midbrain-, and cerebellar-related structures in PD and atypical parkinsonism.^{4,6,8,10,12,14,15,29,34,35,39} The exact location and MR imaging measures in striatal and midbrain-related structures between previous studies and the current study, however, vary.^{34,35,39} This study demonstrated that DTI and $R2^*$ reflect different-yet-complementary information that can be used for discriminating controls and patients with PD, MSA, and PSP. Further refinement of this approach, including the use of novel measures that assess other aspects of disease pathology and the extension to whole-brain feature space, could lead to an optimized tool that can diagnose and differentiate PD from atypical parkinsonism. We envision applying this approach to a large prospective cohort, including a more diverse patient population (PD, MSA, PSP, essential tremor, corticobasal degeneration, and dementia with Lewy bodies), that simulates a real clinical setting to further test its utility in clinical practice.

ACKNOWLEDGMENTS

We thank the MR imaging technical support of Jeffery Vesek and the assistance of study coordinators Melissa Santos and Raghda Clayiff.

Disclosures: Guangwei Du—RELATED: Grant: National Institute of Neurological Disorders and Stroke and Michael J. Fox Foundation for Parkinson's Research.* Michelle M. Lewis—RELATED: Grant: National Institute of Neurological Disorders and Stroke, and Michael J. Fox Foundation for Parkinson's Research UNRELATED: Grants/Grants Pending: National Institute of Environmental Health Sciences*; Travel/Accommodations/Meeting Expenses Unrelated to Activities Listed: Parkinson's Disease Biomarkers Program (PDBP) Annual Consortium Meeting, Comments: every year, the PDBP meets in Bethesda, Maryland, for 1.5 days. The PDBP pays for hotel accommodations, travel, and per diem meals for me to attend the meeting. Nicholas W. Sterling—UNRELATED: Support for Travel to Meetings for the Study or Other Purposes: American Neurological Association, for Parkinson's Research, Comments: every year, the PDBP meets in Bethesda, Maryland, for 1.5 days. The PDBP pays for hotel accommodations, travel, and per diem meals for me to attend the meeting. Nicholas W. Sterling—UNRELATED: Support for Travel to Meetings for the Study or Other Purposes: American Neurological Association, for Parkinson's Research, Comments: I am the coinvestigator on the following grants: National Institutes of Health grant: Multimodal MRI Markers of Nigrostriatal Pathology in Parkinson's Disease; Michael J. Fox Foundation for Parkinson's Research: Benchmark Structural MRI Markers for Parkinsonian Syndromes.* Runze Li—RELATED: Grant: National Science Foundation and National Institutes of Health*; UNRELATED: Grants/Grants Pending: National Science Foundation and National Institutes of Health.* Xuemei Huang—RELATED: Grant: National Institutes of Health, Comments: National Institute of Neurological Disorders and Stroke, and Michael J. Fox Foundation for Parkinson's Research*; UNRELATED: Consultancy: National Institute of Environmental Health Sciences, Comments: This is payment for my consultation for the National Institute of Environmental Health Sciences about Parkinson disease diagnosis; Grants/Grants Pending: National Institute of Environmental Health Sciences, Comments: NIEHS-ES019672.* *Money paid to the institution.

REFERENCES

1. Hughes AJ, Daniel SE, Ben-Shlomo Y, et al. **The accuracy of diagnosis of parkinsonian syndromes in a specialist movement disorder service.** *Brain* 2002;125:861–70 CrossRef Medline
2. Joutsa J, Gardberg M, Røyttä M, et al. **Diagnostic accuracy of parkinsonism syndromes by general neurologists.** *Parkinsonism Relat Disord* 2014;20:840–44 CrossRef Medline
3. Fearnley JM, Lees AJ. **Ageing and Parkinson's disease: substantia nigra regional selectivity.** *Brain* 1991;114(pt 5):2283–301 CrossRef Medline
4. Cykowski MD, Coon EA, Powell SZ, et al. **Expanding the spectrum of neuronal pathology in multiple system atrophy.** *Brain* 2015;138:2293–309 CrossRef Medline
5. Padovani A, Borroni B, Brambati SM, et al. **Diffusion tensor imaging and voxel based morphometry study in early progressive supranuclear palsy.** *J Neurol Neurosurg Psychiatry* 2006;77:457–63 CrossRef Medline
6. Dickson DW, Rademakers R, Hutton ML. **Progressive supranuclear palsy: pathology and genetics.** *Brain Pathol* 2007;17:74–82 CrossRef Medline
7. Blain CR, Barker GJ, Jarosz JM, et al. **Measuring brain stem and cerebellar damage in parkinsonian syndromes using diffusion tensor MRI.** *Neurology* 2006;67:2199–205 CrossRef Medline
8. Nicoletti G, Rizzo G, Barbagallo G, et al. **Diffusivity of cerebellar hemispheres enables discrimination of cerebellar or parkinsonian multiple system atrophy from progressive supranuclear palsy-Richardson syndrome and Parkinson disease.** *Radiology* 2013;267:843–50 CrossRef Medline
9. Prodoehl J, Li H, Planetta PJ, et al. **Diffusion tensor imaging of Parkinson's disease, atypical parkinsonism, and essential tremor.** *Mov Disord* 2013;28:1816–22 CrossRef Medline
10. Focke NK, Helms G, Pantel PM, et al. **Differentiation of typical and atypical Parkinson syndromes by quantitative MR imaging.** *AJNR Am J Neuroradiol* 2011;32:2087–92 CrossRef Medline
11. Lee JH, Han YH, Kang BM, et al. **Quantitative assessment of subcortical atrophy and iron content in progressive supranuclear palsy and parkinsonian variant of multiple system atrophy.** *J Neurol* 2013;260:2094–101 CrossRef Medline

12. Barbagallo G, Sierra-Peña M, Nemmi F, et al. **Multimodal MRI assessment of nigro-striatal pathway in multiple system atrophy and Parkinson disease.** *Mov Disord* 2016;31:325–34 CrossRef Medline
13. Planetta PJ, Ofori E, Pasternak O, et al. **Free-water imaging in Parkinson's disease and atypical parkinsonism.** *Brain* 2016;139(pt 2): 495–508 CrossRef Medline
14. Péran P, Cherubini A, Assogna F, et al. **Magnetic resonance imaging markers of Parkinson's disease nigrostriatal signature.** *Brain* 2010; 133:3423–33 CrossRef Medline
15. Du G, Lewis MM, Styner M, et al. **Combined R2* and diffusion tensor imaging changes in the substantia nigra in Parkinson's disease.** *Mov Disord* 2011;26:1627–32 CrossRef Medline
16. Hughes AJ, Daniel SE, Kilford L, et al. **Accuracy of clinical diagnosis of idiopathic Parkinson's disease: a clinico-pathological study of 100 cases.** *J Neurol Neurosurg Psychiatry* 1992;55:181–84 CrossRef Medline
17. Gilman S, Wenning GK, Low PA, et al. **Second consensus statement on the diagnosis of multiple system atrophy.** *Neurology* 2008;71: 670–76 CrossRef Medline
18. Litvan I, Agid Y, Calne D, et al. **Clinical research criteria for the diagnosis of progressive supranuclear palsy (Steele-Richardson-Olszewski syndrome): report of the NINDS-SPSP international workshop.** *Neurology* 1996;47:1–9 CrossRef Medline
19. Nasreddine ZS, Phillips NA, Bédirian V, et al. **The Montreal Cognitive Assessment, MoCA: a brief screening tool for mild cognitive impairment.** *J Am Geriatr Soc* 2005;53:695–99 CrossRef Medline
20. Avants BB, Tustison NJ, Song G, et al. **A reproducible evaluation of ANTs similarity metric performance in brain image registration.** *Neuroimage* 2011;54:2033–44 CrossRef Medline
21. Wang J, Vachet C, Rumpel A, et al. **Multi-atlas segmentation of subcortical brain structures via the AutoSeg software pipeline.** *Front Neuroinform* 2014;8:7 CrossRef Medline
22. Avants BB, Yushkevich P, Pluta J, et al. **The optimal template effect in hippocampus studies of diseased populations.** *Neuroimage* 2010;49: 2457–66 CrossRef Medline
23. Avants BB, Epstein CL, Grossman M, et al. **Symmetric diffeomorphic image registration with cross-correlation: evaluating automated labeling of elderly and neurodegenerative brain.** *Med Image Anal* 2008;12:26–41 CrossRef Medline
24. Cawley GC, Talbot NL. **On over-fitting in model selection and subsequent selection bias in performance evaluation.** *J Mach Learn Res* 2010;11:2079–107
25. Venkatraman ES. **A permutation test to compare receiver operating characteristic curves.** *Biometrics* 2000;56:1134–38 CrossRef Medline
26. Friedman J, Hastie T, Tibshirani R. **Regularization paths for generalized linear models via coordinate descent.** *J Stat Softw* 2010;33: 1–22 Medline
27. Robin X, Turck N, Hainard A, et al. **pROC: an open-source package for R and S+ to analyze and compare ROC curves.** *BMC Bioinformatics* 2011;12:77 CrossRef Medline
28. Vaillancourt DE, Spraker MB, Prodoehl J, et al. **High-resolution diffusion tensor imaging in the substantia nigra of de novo Parkinson disease.** *Neurology* 2009;72:1378–84 CrossRef Medline
29. Du G, Lewis MM, Sen S, et al. **Imaging nigral pathology and clinical progression in Parkinson's disease.** *Mov Disord* 2012;27:1636–43 CrossRef Medline
30. Schwarz ST, Abaei M, Gontu V, et al. **Diffusion tensor imaging of nigral degeneration in Parkinson's disease: a region-of-interest and voxel-based study at 3 T and systematic review with meta-analysis.** *Neuroimage Clin* 2013;3:481–88 CrossRef Medline
31. Lewis MM, Du G, Kidacki M, et al. **Higher iron in the red nucleus marks Parkinson's dyskinesia.** *Neurobiol Aging* 2013;34:1497–503 CrossRef Medline
32. He N, Ling H, Ding B, et al. **Region-specific disturbed iron distribution in early idiopathic Parkinson's disease measured by quantitative susceptibility mapping.** *Hum Brain Mapp* 2015;36: 4407–20 CrossRef Medline
33. Schocke MF, Seppi K, Esterhammer R, et al. **Diffusion-weighted MRI differentiates the Parkinson variant of multiple system atrophy from PD.** *Neurology* 2002;58:575–80 CrossRef Medline
34. Tsukamoto K, Matsusue E, Kanasaki Y, et al. **Significance of apparent diffusion coefficient measurement for the differential diagnosis of multiple system atrophy, progressive supranuclear palsy, and Parkinson's disease: evaluation by 3.0-T MR imaging.** *Neuroradiology* 2012;54:947–55 CrossRef Medline
35. Seppi K, Schocke MF, Esterhammer R, et al. **Diffusion-weighted imaging discriminates progressive supranuclear palsy from PD, but not from the parkinson variant of multiple system atrophy.** *Neurology* 2003;60:922–27 CrossRef Medline
36. Salvesen L, Ullerup BH, Sunay FB, et al. **Changes in total cell numbers of the basal ganglia in patients with multiple system atrophy: a stereological study.** *Neurobiol Dis* 2015;74:104–13 CrossRef Medline
37. Betts MJ, Acosta-Cabronero J, Cardena-Blanco A, et al. **High-resolution characterisation of the aging brain using simultaneous quantitative susceptibility mapping (QSM) and R2* measurements at 7T.** *Neuroimage* 2016;138:43–63 CrossRef Medline
38. Minnerop M, Specht K, Ruhlmann J, et al. **Voxel-based morphometry and voxel-based relaxometry in multiple system atrophy—a comparison between clinical subtypes and correlations with clinical parameters.** *Neuroimage* 2007;36:1086–95 CrossRef Medline
39. Rizzo G, Martinelli P, Manners D, et al. **Diffusion-weighted brain imaging study of patients with clinical diagnosis of corticobasal degeneration, progressive supranuclear palsy and Parkinson's disease.** *Brain* 2008;131:2690–700 CrossRef Medline
40. Zanigni S, Calandra-Buonaura G, Manners DN, et al. **Accuracy of MR markers for differentiating progressive supranuclear palsy from Parkinson's disease.** *Neuroimage Clin* 2016;11:736–42 CrossRef Medline
41. Stutzbach LD, Xie SX, Naj AC, et al. **The unfolded protein response is activated in disease-affected brain regions in progressive supranuclear palsy and Alzheimer's disease.** *Acta Neuropathol Commun* 2013;1:31 CrossRef Medline
42. Dickson DW. **Parkinson's disease and parkinsonism: neuropathology.** *Cold Spring Harb Perspect Med* 2012;2:a009258 Medline
43. Agosta F, Pievani M, Svetel M, et al. **Diffusion tensor MRI contributes to differentiate Richardson's syndrome from PSP-parkinsonism.** *Neurobiol Aging* 2012;33:2817–26 CrossRef Medline
44. Boelmans K, Holst B, Hackius M, et al. **Brain iron deposition fingerprints in Parkinson's disease and progressive supranuclear palsy.** *Mov Disord* 2012;27:421–27 CrossRef Medline
45. Massey LA, Jäger HR, Paviour DC, et al. **The midbrain to pons ratio: a simple and specific MRI sign of progressive supranuclear palsy.** *Neurology* 2013;80:1856–61 CrossRef Medline
46. Focke NK, Helms G, Scheewe S, et al. **Individual voxel-based subtype prediction can differentiate progressive supranuclear palsy from idiopathic Parkinson syndrome and healthy controls.** *Hum Brain Mapp* 2011;32:1905–15 CrossRef Medline
47. Buchman AS, Leurgans SE, Yu L, et al. **Incident parkinsonism in older adults without Parkinson disease.** *Neurology* 2016;87:1036–44 CrossRef Medline
48. Wang Y, Liu T. **Quantitative susceptibility mapping (QSM): Decoding MRI data for a tissue magnetic biomarker.** *Magn Reson Med* 2015;73:82–101 CrossRef Medline
49. Ofori E, Pasternak O, Planetta PJ, et al. **Increased free water in the substantia nigra of Parkinson's disease: a single-site and multi-site study.** *Neurobiol Aging* 2015;36:1097–104 CrossRef Medline
50. Massey LA, Micallef C, Paviour DC, et al. **Conventional magnetic resonance imaging in confirmed progressive supranuclear palsy and multiple system atrophy.** *Mov Disord* 2012;27:1754–62 CrossRef Medline
51. Reiter E, Mueller C, Pinter B, et al. **Dorsolateral nigral hyperintensity on 3.0T susceptibility-weighted imaging in neurodegenerative Parkinsonism.** *Mov Disord* 2015;30:1068–76 CrossRef Medline
52. Scherfler C, Göbel G, Müller C, et al. **Diagnostic potential of automated subcortical volume segmentation in atypical parkinsonism.** *Neurology* 2016;86:1242–49 CrossRef Medline